

# Toward a Simulation Approach for Alkene Ring-closing Metathesis: Scope and Limitations of a Model for RCM

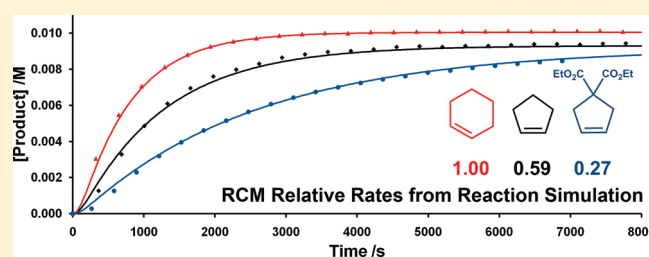
David J. Nelson,<sup>†</sup> Davide Carboni,<sup>†,‡</sup> Ian W. Ashworth,<sup>§</sup> and Jonathan M. Percy<sup>\*,†</sup>

<sup>†</sup>WestCHEM, Department of Pure and Applied Chemistry, University of Strathclyde, 295 Cathedral Street, Glasgow, G1 1XL, United Kingdom

<sup>§</sup>AstraZeneca Pharmaceutical Development, Silk Road Business Park, Charter Way, Macclesfield, SK10 2NA, United Kingdom

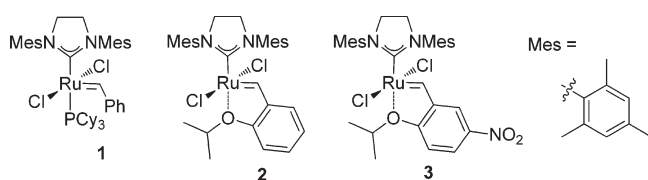
**S** Supporting Information

**ABSTRACT:** A published model for revealing solvent effects on the ring-closing metathesis (RCM) reaction of diethyl diallylmalonate **7** has been evaluated over a wider range of conditions, to assess its suitability for new applications. Unfortunately, the model is too flexible and the published rate constants do not agree with experimental studies in the literature. However, by fixing the values of important rate constants and restricting the concentration ranges studied, useful conclusions can be drawn about the relative rates of RCM of different substrates, precatalyst concentration can be simulated accurately and the effect of precatalyst loading can be anticipated. Progress has also been made toward applying the model to precatalyst evaluation, but further modifications to the model are necessary to achieve much broader aims.



## INTRODUCTION

The alkene ring-closing metathesis (RCM) reaction has enabled many complex and important molecules to be constructed in new ways. The popularity of the RCM reaction has been driven by the commercial availability of highly active and stable ruthenium precatalysts such as **1–3**.



Industry has seized upon the potential of the technology, and reactions have now progressed from the realm of the discovery chemist<sup>1</sup> into chemical development and scale-up.<sup>2–4</sup> The Boehringer-Ingelheim group have prepared BILN 2061 **4** on a multikilogram scale using RCM of diene **5** to form 15-membered macrocycle **6** as a key step (Scheme 1).

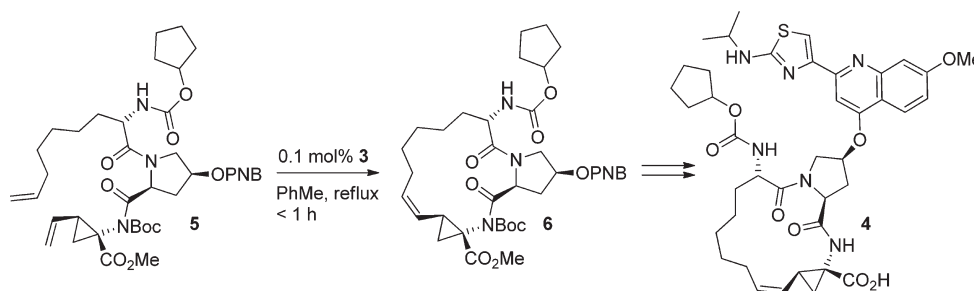
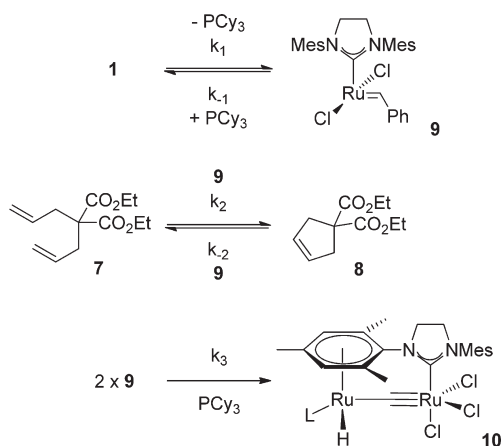
During the course of the campaign, extensive optimization studies involving changes of solvent, precatalyst and substrate structure were carried out, and cyclization efficiency was quantified using the method described by Ercolani et al.;<sup>5</sup> plotting the concentration of cyclic product squared versus the concentration of cyclic dimer yields a linear plot with slope  $(EM_{\text{product}})^2 / (EM_{\text{dimer}})$  (eq 1), which can be used to compare different reaction conditions quantitatively.

$$[\text{product}]^2 / [\text{cyclicdimer}] = (EM_{\text{product}})^2 / (EM_{\text{dimer}}) \quad (1)$$

The study showed that the quantification of reaction outcomes required some care, as the process of product isolation can change the reaction yield unless all the metathesis-active species are quenched before samples are concentrated.<sup>6</sup> The increasing concentration during solvent removal can result in secondary metathesis events that may be complex in nature<sup>2</sup> and demonstrates the difficulty involved in using reaction yields from the synthetic chemistry literature to draw firm conclusions about the interplay between structure and reactivity. We have used <sup>1</sup>H NMR, a less invasive method, to quantify the outcomes of small-scale metathesis reactions of simple  $\alpha,\omega$ -dienes<sup>7</sup> and to follow the course of their RCM reactions in kinetic studies.<sup>8</sup> We have also modeled the potential energy surfaces for these reactions in some detail using the M06-L functional.<sup>9</sup> It should be possible to interpret the concentration/time data obtained from kinetic experiments using a combination of computational insights and quantitative data obtained from fundamental studies of precatalyst systems. An appropriate kinetic model that takes account of precatalyst initiation and active catalyst decomposition would allow the interpretation of this concentration/time data (which very rarely correspond to a simple kinetic order<sup>8</sup>) and comparisons between different reaction solvents and precatalyst systems. The 2008 study published by Adjiman, Taylor and co-workers was therefore of great interest.<sup>10</sup> The study applied a very simple kinetic model to the cyclization of diethyl diallylmalonate **7** to form product **8** (using Grubbs second generation precatalyst **1**) and promoted acetic acid as an unexpectedly effective solvent for

Received: August 4, 2011

Published: September 14, 2011

Scheme 1. <sup>4</sup>Scheme 2. <sup>10</sup>

RCM reactions on the basis of the findings; the model took account of precatalyst initiation and active catalyst decomposition explicitly (Scheme 2,  $L = H_2IMes$ ). The model comprises reversible initiation of **1** to form 14e benzylidene **9**, reversible RCM of **7** to form **8** and irreversible decomposition of two molecules of **9** to form **10**. Numerical integration software was used to analyze and simulate concentration/time data from reactions<sup>11</sup> that were carried out under reaction conditions similar to those used for the majority of target synthesis projects.

The meticulous exclusion of oxygen and water from reactions using glovebox techniques is required for maximum rigor, but such procedures bear almost no resemblance to the way RCM reactions are carried out in the synthetic laboratory. Indeed, the relative robustness of ruthenium-based precatalysts represents one of the reasons for their wide appeal and ubiquity compared to the more active but far more fragile molybdenum-based systems. While synthetic chemists would use dried (and typically degassed) solvents, they would not usually do more, so the level of rigor employed by Adjiman, Taylor and co-workers is entirely appropriate and relevant. If their model could be applied to other systems, it could be used by synthetic chemists to predict conditions under which maximum reaction yield could be obtained at optimal substrate concentration, with the most appropriate precatalyst at the lowest practical loading and reaction time, with obvious and considerable advantages to those involved in scale-up campaigns. We therefore set out to apply the published model to our own systems of interest and investigate its scope and limitations; we report our findings in this manuscript.

## RESULTS AND DISCUSSION

Reaction concentration/time data were collected for the RCM reactions of diethyl diallylmalonate **7** to form product **8**, heptadiene **11** to form cyclopentene **12** and octadiene **13** to form cyclohexene **14** (Scheme 3) catalyzed by **1** and **2**, by <sup>1</sup>H NMR (at 400 or 600 MHz) following the procedures described previously.<sup>8</sup>

Dichloromethane-*d*<sub>2</sub> (DCM-*d*<sub>2</sub>) was used initially as it is the default solvent for synthetic RCM; however, we also used chloroform-*d* for many experiments because it is a fraction of the cost of DCM-*d*<sub>2</sub> and precatalyst initiation occurs at similar rates in the two solvents (*vide infra*). Stock solutions of substrates and precatalysts were prepared in dried solvents (solvents were allowed to stand over activated 4 Å molecular sieves overnight, then degassed before use by sparging with dry oxygen-free nitrogen) using dried volumetric glassware so that weighing and dilution errors would be minimized. For more dilute reactions, concentrated stock solutions were prepared and diluted down immediately before use. Solid **1** and **2** and their solutions were handled with care under a flow of nitrogen. Reactions were carried out in NMR tubes fitted with pierced caps, allowing free egress of ethene. The published model (Scheme 2, eqs 2–6)<sup>10</sup> was constructed in both Berkeley Madonna<sup>12</sup> and Micromath Scientist<sup>13</sup> software packages (using the default Runge–Kutta fourth-order integration method for each)<sup>14</sup> and reaction concentration/time data (for dienes **7**, **11** and **13** and products **8**, **12** and **14**) were imported as text files or spreadsheets, respectively. Each experiment was checked for mass balance: the reactions treated in this manuscript all convert diene to cycloalkene (plus ethene) without the formation of oligomers or side-products.<sup>7</sup>

Initially, attempts were made to reproduce the experiment in DCM-*d*<sub>2</sub> reported by Adjiman and Taylor (120 mM **7**, 6.7 mM **1**) and obtain the published rate constants through fitting.

$$\frac{d}{dt}[1] = k_1[1] + k_{-1}[9][PCy_3] \quad (2)$$

$$\frac{d}{dt}[9] = k_1[1] + k_{-1}[9][PCy_3] - 2k_3[9] \quad (3)$$

$$\frac{d}{dt}[PCy_3] = k_1[1] + k_{-1}[9][PCy_3] - k_3[9] \quad (4)$$

$$\frac{d}{dt}[7] = k_2[7][9] + k_{-2}[8][9] \quad (5)$$

$$\frac{d}{dt}[8] = k_2[7][9] - k_{-2}[8][9] \quad (6)$$

Unfortunately, the concentration/time profile recorded indicated a faster reaction than the one published (Figure 1). A slower reaction took place in DCM-*d*<sub>2</sub> from a freshly opened ampule, although this did not match the literature concentration/time profile either. Karl Fischer titration showed that the

Scheme 3

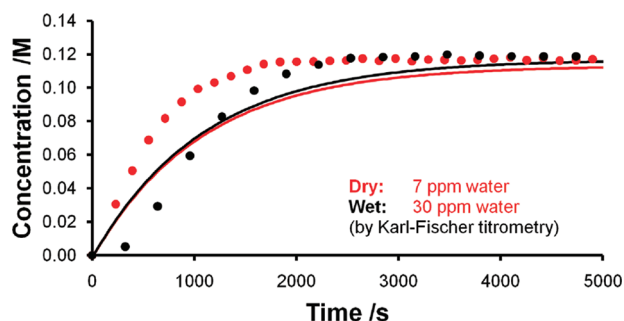
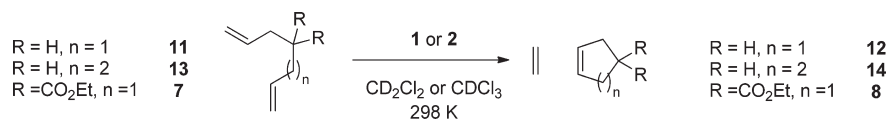


**Figure 1.** Experimental concentration/time data and simulations thereof obtained using the Adjiman and Taylor model and rate constants for the RCM of **7** in dry DCM- $d_2$  (red ●, red line) and wet DCM- $d_2$  (●, black line) at 298 K. Diene and cycloalkene concentration were both fitted, but only cycloalkene concentration is shown for clarity.

**Table 1.** Rate Constants ( $\text{L mol}^{-1} \text{s}^{-1}$ ) Used to Obtain a Good Fit of the 120 mM Data Set, Plus Those Reported for the RCM of **7** in DCM- $d_2$

entry	reference	$k_1$	$k_{-1}$	$k_2$	$k_{-2}$	$k_3$
1	This work	0.000394 <sup>b</sup>	19.8	5.39	0.0529	$3.28 \times 10^{-6}$
2	Adjiman et al. <sup>a</sup>	0.0617	0.373	0.137	0.00775	0

<sup>a</sup> From reference.<sup>10</sup> <sup>b</sup> Units  $\text{s}^{-1}$ .

drying procedure had been effective, with a water content of *ca.* 30 ppm before drying (untreated chloroform- $d$  and DCM- $d_2$ ) but less than 10 ppm afterward. It is clear that commercial NMR solvents from ampoules must be treated with some caution if relatively significant amounts of water are not to be introduced. Straightforward drying of solvents using molecular sieves reduced the water content of the deuterated solvents to a level similar to that found in DCM obtained from widely used solvent purification systems; for example, DCM from the Innovative Technologies PureSolv system used in-house contains water at no more than 5 ppm. Although the kinetic data were not consistent with the published literature profile, we fitted the data set; diene and cycloalkene concentration were both fitted, but only cycloalkene concentration is shown for clarity. An excellent fit was obtained for both species. However, quite different values for all rate constants were required (Table 1), prompting further investigation with this data set.

Diethyl diallylmalonate **7** is used as a benchmark substrate to assess the performance of new precatalyst systems<sup>15</sup> because it is assumed to cyclize irreversibly and *via* rate-limiting precatalyst initiation.<sup>16,17</sup> The absolute values of  $k_1$  and  $k_{-1}$  should be very influential on the predicted concentration/time profiles, so the value of  $k_1$  was stepped in factors of 10 between fixed values from  $10^{-10}$  to  $10^{-2} \text{s}^{-1}$  in the fitting, allowing  $k_2$  and  $k_{-2}$  to optimize. The  $k_2$  and  $k_{-2}$  constants represent many events comprising the ring-closing metathesis process; this is an inherent weakness in a

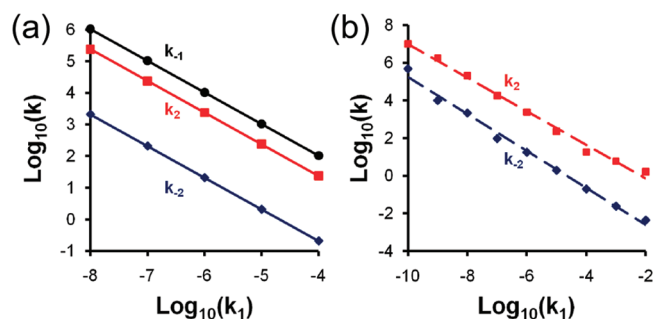


**Figure 2.** Testing the flexibility of  $k_1$  in the model with (a)  $k_3$  fixed to zero and with (b)  $k_3$  allowed to change in the fitting routine.

fitting approach but it represents one way to achieve significant simplification without recourse to unrealistic reaction conditions. The fitting was carried out twice: once where  $k_3$  (catalyst decomposition) was fixed to zero and once where  $k_3$  was allowed to vary in the fitting. Good fits were obtained for all values of  $k_1$  from  $10^{-8}$  to  $10^{-4} \text{s}^{-1}$  when  $k_3$  was fixed, and from  $10^{-10}$  to  $10^{-2} \text{s}^{-1}$  when  $k_3$  was allowed to change, which is very surprising given the importance of precatalyst activation. The values of other rate constants changed smoothly with changes in  $k_1$  (Figure 2).

It is clear these rate constants are correlated; the model will tolerate quite large changes in  $k_1$  by readjusting the value of other rate constants in direct proportion to the change in  $k_1$ , because the rate constants in the model are all dependent on  $k_1$ . The irrelevance of the absolute value of  $k_1$  is a source of considerable concern; *unconstrained* fitting of even moderately complex reactions is unwise because of the number of variables and the dependencies between them. The absolute values of strongly correlated rate constants cannot be obtained from fitting.

With these results in hand, concentration/time data were recorded for the RCM reactions of diethyl diallylmalonate **7** over a range of reaction conditions (10 to 500 mM **7**, 1 to 10 mol % **1**, Table 2).

Multiple data sets were imported into Berkeley Madonna and fitted simultaneously (batch fitted) to the Adjiman model, on the basis that fitting a number of the data sets in Table 2 would yield a set of rate constants that could describe a wider range of conditions. Unfortunately, a fit that described all data sets at once could not be achieved through this batch fitting approach. The rate constants corresponding to the best fit are in Table 3.

While the best fit described the shapes of the concentration/time profiles well for some data sets (where  $[\mathbf{7}] \geq 250 \text{ mM}$ ), fitting of the experimental data was moderate or poor for others. Figure 3 shows excellent ( $[\mathbf{7}] = 500 \text{ mM}$ ), moderate ( $[\mathbf{7}] = 120 \text{ mM}$ ) and poor ( $[\mathbf{7}] = 50 \text{ mM}$ ) fits from the batch fitting results. We refer to the maximum difference between experimental and simulated concentrations during the reaction. At this point, it is clear that the flexibility of the model with respect to diene concentration is a major limitation; at a given diene concentration, precatalyst concentration can be varied with good fits obtaining (*vide infra*). Different best fits can be found for each

Table 2. Conditions Explored for the RCM Reactions of 7

data set	[7] <sup>a</sup>	[1] <sup>a</sup>	loading of 1 <sup>a</sup>
1	505.9 mM (500 mM)	25.7 mM (25 mM)	5.1 mol % (5.0 mol %)
2	491.7 mM (500 mM)	12.0 mM (12.5 mM)	2.4 mol % (2.5 mol %)
3	507.0 mM (500 mM)	5.2 mM (5 mM)	1.0 mol % (1.0 mol %)
4	404.5 mM (400 mM)	14.4 mM (14 mM)	3.6 mol % (3.5 mol %)
5	250.7 mM (250 mM)	25.9 mM (25 mM)	10.3 mol % (10.0 mol %)
6	250.5 mM (250 mM)	12.7 mM (12.5 mM)	5.1 mol % (5.0 mol %)
7 <sup>b</sup>	121.7 mM (120 mM)	6.7 mM (6.7 mM)	5.5 mol % (5.6 mol %)
8 <sup>b</sup>	121.8 mM (120 mM)	6.7 mM (6.7 mM)	5.5 mol % (5.6 mol %)
9 <sup>b,c</sup>	119.6 mM (120 mM)	6.7 mM (6.7 mM)	5.6 mol % (5.6 mol %)
10	76.1 mM (75 mM)	1.2 mM (1.1 mM)	1.6 mol % (1.5 mol %)
11	50.2 mM (50 mM)	5.1 mM (5 mM)	10.1 mol % (10.0 mol %)
12	48.2 mM (50 mM)	1.2 mM (1.3 mM)	2.5 mol % (2.5 mol %)
13	9.9 mM (10 mM)	0.1 mM (0.1 mM)	mol % (1.0 mol %)

<sup>a</sup> Nominal values in parentheses. <sup>b</sup> Conditions used by Adjiman et al.<sup>10</sup>

<sup>c</sup> Kinetic data collected using <sup>1</sup>H NMR at 600 MHz with 2 scans per data point.

Table 3. Rate Constants (L mol<sup>-1</sup> s<sup>-1</sup>) Obtained from Batch-Fitting 13 RCM Reaction Concentration/Time Profiles to the Model in Scheme 2

k <sub>1</sub> <sup>a</sup>	k <sub>-1</sub>	k <sub>2</sub>	k <sub>-2</sub>	k <sub>3</sub>
1.64 × 10 <sup>-5</sup>	243	64.1	0.890	0.567

<sup>a</sup> Units s<sup>-1</sup>.

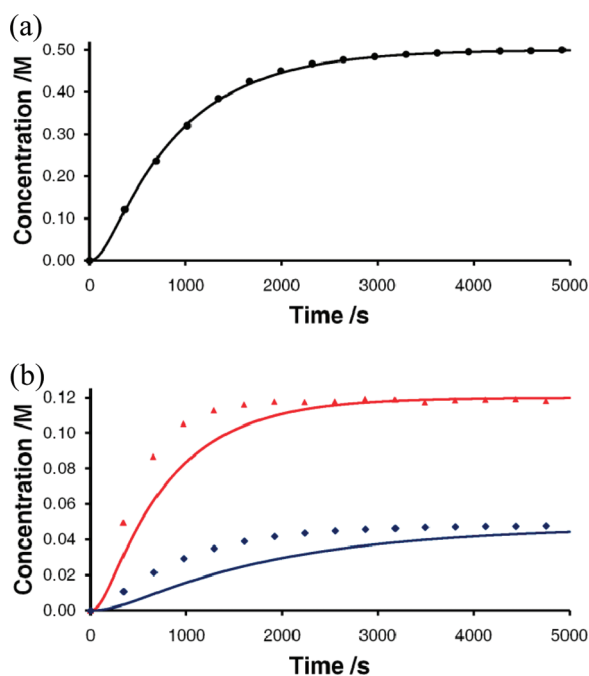
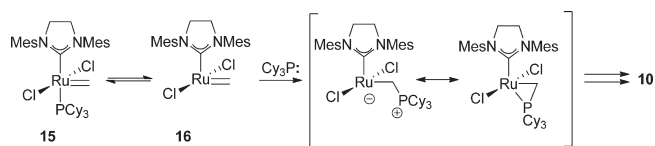


Figure 3. Testing the quality of fitting as a function of diene concentration for (a) [7] = 500 mM (1 mol % 1) (● = data points, solid line = simulation) and (b) [7] = 120 mM (5.5 mol % 1) (▲, red solid line) and [7] = 50 mM (2.5 mol % 1) (blue ◆, blue solid line).

data set; either these are not *global* but *local* minima, or the model simply fails to describe a range of conditions.

Scheme 4.<sup>24</sup>

Attention then turned to constraining the value of  $k_1$  in the fitting, reflecting the importance of the precatalyst initiation event. The kinetics of the initiation of precatalysts **1**, **2** and **3** have been studied in some depth<sup>18–20</sup> and the initiation rate of **2** in DCM at 298 K is already known (0.0263 L mol<sup>-1</sup> s<sup>-1</sup>).<sup>20</sup>

Values of  $1.40 \times 10^{-4}$  and  $4.5 \times 10^{-5}$  s<sup>-1</sup> were obtained for **1** in DCM and chloroform, respectively, and 0.0234 L mol<sup>-1</sup> s<sup>-1</sup> for **2** in chloroform (see the Supporting Information for details) by following the reaction of the precatalyst with ethyl vinyl ether at 298 K by either <sup>1</sup>H NMR (for **1**) or UV/vis spectroscopy (for **2**). These modest differences in initiation rate render chloroform-*d* a cost-effective solvent for the study of RCM.

Though the 14e complex **9** is an accepted intermediate on the energy surfaces for metathesis pathways, the barriers to alkene coordination or phosphane recoordination are very small.<sup>21,22</sup> The value of  $k_{-1}/k_2$  (where  $k_2$  refers to the rate of alkene coordination) is close to 1 from the experimental work of Sanford et al., consistent with similar barriers for both pathways.<sup>18</sup> However, complex **9** undergoes barrierless forward and backward reactions, so it follows that  $k_1/k_{-1}$  should reflect this in a very low numerical value. The absolute value of  $K$  for the initiation therefore derives from the *ca.* 25 kcal mol<sup>-1</sup> energy for Ru–P bond separation;  $k_1/k_{-1} = K \approx 10^{-19}$  at 298 K follows from this. The ratios of  $k_1/k_{-1}$  derived by Adjiman and Taylor ( $k_1/k_{-1} = 0.18$  in dichloromethane, Table 1) are therefore inconsistent with detailed experimental and theoretical studies on the phosphane dissociation event.

The values of  $k_3$ , which represent the rate of a bimolecular decomposition of active catalyst, also varied considerably with solvent.<sup>10</sup> According to the work of Hong et al., phosphane-bound methylidene **15** decomposes *via* 14e methylidene **16** to yield diruthenium complex **10** (Scheme 4);<sup>23,24</sup> two molecules of **16** and one of tricyclohexylphosphane are consumed to produce one molecule of **10**, with tricyclohexylphosphane being converted to tricyclohexylphosphonium chloride in the process.

In the Adjiman model, this pathway is represented by the term  $k_3[9]^2$ , but inspection of the high-field region of the <sup>1</sup>H NMR spectrum of a 500 mM RCM of **7** (2.5 mol % **1**) did not reveal **10**, whereas **1** and **15** are clearly visible. Formation of the diruthenium hydride complex **10** has been observed in concentrated solutions (>20 mM) of phosphane-bound methylidene **15** at higher temperatures (322 K), or in the presence of a large excess of ethene, so the formation of **10** (which requires two bimolecular steps) would be expected to be slow under the mild and more dilute conditions used here and in most synthetic RCM experiments. The decomposition pathway characterized by Hong et al. has not yet been shown to account for significant quantities of ruthenium-carbene loss in synthetic RCM experiments.

The value of  $k_1$  was then fixed to the experimentally determined value (for the relevant precatalyst/solvent combination) for subsequent fitting. Simultaneous fitting of the 13 RCM reaction concentration/time profiles (with  $k_3$  fixed to zero) in Table 2 yielded a new set of rate constants (Table 4). Once again, these rate constants failed to describe a range of concentrations



and only described reactions well when  $[7] \geq 250$  mM. At this point, the limitations appear to follow from the way in which the model is constructed (that is, the differential equations used to set it up).

The literature model was also constructed in Micromath Scientist, which provides a number of useful statistics with which to evaluate and compare reaction models, in order to evaluate how flexible the model was with a fixed value for  $k_1$ .<sup>13</sup> Three data sets covering a wide concentration range (entries 3, 7, and 12 in Table 2) were fitted to the model in turn, providing good fits in each case but requiring vastly different rate constants (entries 1, 2, and 3 in Table 5).

Analysis of the fitting statistics showed that all rate constants were highly correlated, in agreement with the previous result (Figure 2), and that 95% confidence limits for each rate constant were very wide indeed. The confidence limits for  $k_3$  are so wide (and encompass zero) as to suggest that its value has very little bearing on the reaction, as would be expected for a bimolecular process occurring under very dilute conditions. Attempts at fitting multiple data sets using Scientist were unsuccessful; fitting the three data sets which had been examined separately yielded a good fit for the 500 mM reaction but underestimated the rates of the 120 and 50 mM reactions by *ca.* 30 and 50%, respectively (entry 4 in Table 5).

It is now useful to examine the model in more detail, understand more fully the importance of  $k_1$  and identify the scope and utility of the model in its current form. One of the important predictions of Adjiman, Taylor and co-workers concerns the extent to which precatalyst **1** dissociates, and the concentration/time profile of active catalyst **9**. The published paper does not report any measurements of the concentration of **1**, even though the solution concentration would have allowed the benzyldiene proton to be observed ( $\delta_{\text{H}} = \text{ca. } 19.2$  ppm in chloroform-*d* and DCM-*d*<sub>2</sub>)<sup>25</sup> and integrated with confidence. When spectra were recorded over a 20 ppm chemical shift range, the change in concentration of **1** was seen to be modest during the course of the reaction. Most of the initial charge of **1** remains well after complete conversion of **7** to **8**, in agreement with previous literature reports,<sup>26</sup> indicating clearly that the reaction conditions are not causing extensive catalyst decomposition on the time scale of the RCM (Figure 4).

Complete dissociation of phosphane clearly does not occur; the simulated catalyst concentration/time profile presented by

**Table 4.** Rate Constants ( $\text{L mol}^{-1} \text{s}^{-1}$ ) Obtained from Batch-Fitting 13 RCM Reaction Concentration/Time Profiles to the Model in Scheme 2, Fixing  $k_1$  to  $1.4 \times 10^{-4} \text{ s}^{-1}$  and  $k_3$  to  $0 \text{ L mol}^{-1} \text{ s}^{-1}$

$k_1^{a,b}$	$k_{-1}$	$k_2$	$k_{-2}$	$k_3^a$
$1.4 \times 10^{-4}$	29.8	7.69	0.110	0

<sup>a</sup> Value fixed. <sup>b</sup> Units  $\text{s}^{-1}$ .

**Table 5.** Rate Constants ( $\text{L mol}^{-1} \text{s}^{-1}$ ) Obtained through Fitting Data Sets in Micromath Scientist; Error Bars Are 95% Confidence Intervals

entry	data set(s)	$k_{-1}$	$k_2$	$k_{-2}$	$k_3$
1	3	$23.4 \pm 5.9$	$7.19 \pm 0.525$	$0.0394 \pm 0.0011$	$0.461 \pm 0.501$
2	7	$28.8 \pm 11.5$	$13.9 \pm 1.95$	$0.213 \pm 0.0797$	$1.42 \times 10^{-14} \pm 9.41 \times 10^{-13}$
3	12	$166 \pm 61$	$35.9 \pm 5.1$	$0.195 \pm 0.118$	$0.0308 \pm 2.3763$
4	3, 7, 12	$27.4 \pm 14.5$	$7.99 \pm 1.30$	$0.0452 \pm 0.0271$	$0.621 \pm 1.049$

Adjiman and Taylor is an artifact arising from the use of an excessively large value of  $k_1$  ( $6.17 \times 10^{-2} \text{ s}^{-1}$ ).

A second alkylidene species was observed to form slowly during RCM reactions, with a chemical shift consistent with metathesis inactive methylidene complex **15** ( $\delta_{\text{H}} = 17.8$  ppm), formed by irreversible recapture of **16** by phosphane;<sup>18</sup> despite recent and detailed low-temperature NMR studies by van der Eide,<sup>27</sup> **16** has not yet been detected by NMR. Capture of **16** by phosphane is slow because the concentrations of **16** and phosphane are very low; substrates, ethene and products, all competitive and reversibly binding ligands, are all present at much higher concentrations. In the reaction profile in Figure 4, complete turnover of **7** has been achieved at the expense of *ca.* 30% of the original charge of **1**; of this, *ca.* 15% appears as **15** so an equal amount (*ca.* 15%) of the original charge of **1** remains unaccounted for. The continued decrease in the concentration of precatalyst **1** even after the reaction has finished is due to reaction with ethene, which is known to yield a low energy metallocyclobutane after reaction with two molecules of ethene.<sup>28</sup> This initiation behavior was confirmed by following the decay of the precatalyst **1** in ethene-sparged solvent, which occurred at the same rate as precatalyst initiation with ethyl vinyl ether.

Adjiman and Taylor present a simulation of active catalyst concentration which shows rapid and complete precatalyst dissociation followed by active catalyst decomposition at various rates in each solvent,<sup>10</sup> which is not consistent with experimental observations. For each of the reactions in Table 2, the precatalyst concentration after approximately 2000 s was measured by <sup>1</sup>H NMR integration and compared to the values obtained at the same time point using simulations with rate constants from Adjiman and Taylor, or using our best fit set of rate constants from Table 4 (Figure 5).

It can be concluded that the rate constants in Table 4 represent the behavior of the precatalyst more effectively, but still do not completely account for its behavior in RCM reactions. Various values of  $k_{-1}$ ,  $k_2$  and  $k_{-2}$  can still be obtained, depending on which data set is fitted, presumably due to the large number of

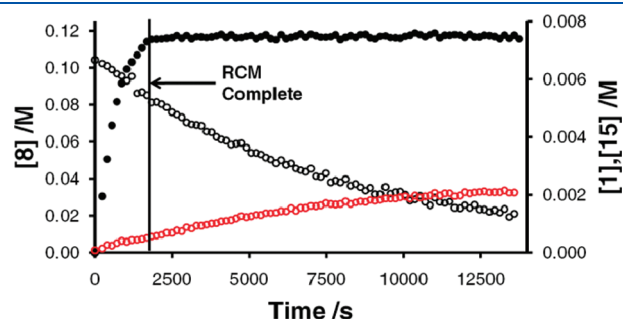


**Figure 4.** Concentration/time profiles of **8** (●), precatalyst **1** (○) and inactive phosphane-bound methylidene **13** (red ○) during the RCM of **7** (120 mM, 5.5 mol % **1**; entry 9 in Table 2).

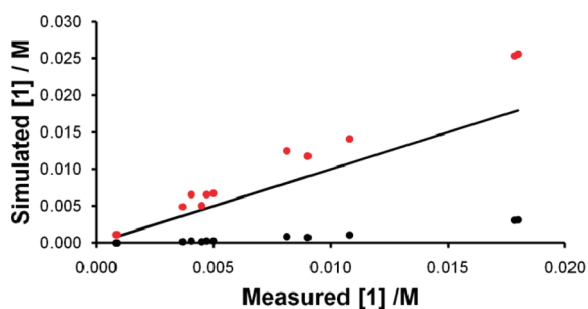


**Figure 5.** Plot of simulated versus measured [1] after *ca.* 2000 s in experiments in Table 2 (except data set 13) using (a) rate constants in Table 1, entry 2 (●) or (b) rate constants in Table 4 (red ●); the black line represents identity between simulated and measured values (i.e., slope = 1).

**Table 6.** Rate Constants ( $\text{L mol}^{-1} \text{s}^{-1}$ ) Used to Describe RCM of 7 Across Defined Concentration Ranges

entry	[7] range	$k_{-1}$	$k_2$	$k_{-2}$
1	250–500 mM	26.6	6.90	0.103
2	50–120 mM	71.1	20.0	0.165

local minima for the fitting method. Further changes to the model are required before a wide range of concentrations can be described.

Attempts were therefore made to fit multiple data sets within a narrower range of concentrations and explore the concentration range over which the approximations and simplifications of the model hold. Rate constants were obtained (through data fitting) that describe all experiments with 250–500 mM 7 (Table 6, entry 1; data sets 1 to 6 in Table 2) and a second set that describe all experiments with 50–120 mM 7 (Table 6, entry 2; data sets 7 to 12 in Table 2);  $k_1$  and  $k_3$  were fixed in the fitting. Examples of the fits obtained can be found in Figure 6.

There are clear differences between the rate constants required to fit the different concentration regimes, with higher  $k_{-1}$  and  $k_2$  values required to successfully model the lower concentration reactions. The different value of  $k_{-1}$  is required due to the incorrect modeling of the 14e species (methylidene 16 does not capture phosphane reversibly) and the absence of ethene from the reaction model means that [ethene] is effectively embedded in  $k_{-2}$ . However, the rate constants successfully fit different pre-catalyst loadings and substrate concentrations within these ranges and are therefore useful for predicting the effect of changing these parameters, for example, to predict the lowest loading of 1 that will effect complete reaction within a given time frame.

The extraction of rate constants for different substrates was the original aim of this project, so attention turned to assessing different substrates in RCM reactions quantitatively from reactions conducted at the same initial diene concentration. Concentration/time data for the RCM of 7 (Table 2, data set 13), heptadiene 11 to form cyclopentene (in duplicate) and octadiene 12 (in duplicate) in DCM- $d_2$ , all with 10 mM substrate and 0.1 mM 1, were imported into Berkeley Madonna and fitted to the simple model in Scheme 2. The values of  $k_1$  ( $1.4 \times 10^{-4} \text{s}^{-1}$ ) and  $k_3$  (zero) were fixed and the data was fitted with a common  $k_1$ ,  $k_{-1}$  and  $k_3$  (substrate independent rate constants) but a different  $k_2$  and  $k_{-2}$  for each substrate. The rate constants in Table 7 and the fit in Figure 7 were obtained.

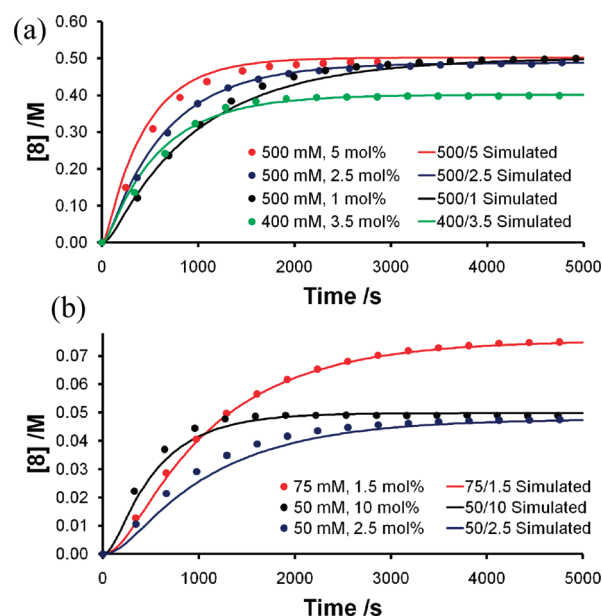


**Figure 6.** Rate constants in Table 6 describe experiments at (a) 500 mM, using entry 1, and (b) 50 mM, using entry 2, relatively well, even when the pre-catalyst concentration varies.

**Table 7.** Rate Constants ( $\text{L mol}^{-1} \text{s}^{-1}$ ) Obtained from Fitting Concentration/Time Data for Heptadiene 11, Octadiene 13 and Diethyl Diallylmalonate 7 RCM Reactions Simultaneously

diene	$k_{-1}$	$k_2$	$k_{-2}$	$k_{\text{rel}}^a$
11		359	11.6	0.589
12	2733	610	3.32	1.000
7		166	13.1	0.272

<sup>a</sup> Calculated by dividing  $k_2$  for that substrate by  $k_2$  for octadiene RCM.

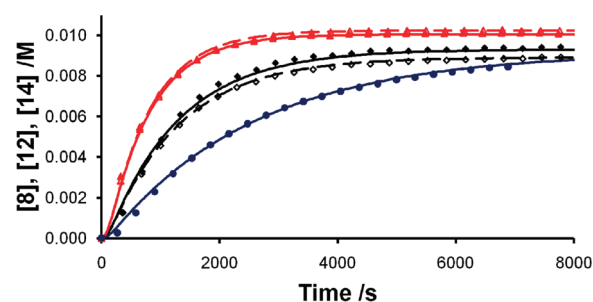


**Figure 7.** Fitting concentration/time data for the RCM reactions of heptadiene (◆ = data points, solid black line = simulation; ◇, dashed black line), octadiene (red ▲, solid red line and red △, dashed red line) and diethyl diallylmalonate (blue ●, solid blue line); the initial substrate concentration was 10 mM (1 mol % 1).

The model is therefore useful for deriving quantitative conclusions about the relative rate of RCM of different substrates. Interestingly, the RCM of diethyl diallylmalonate appears to occur at half the rate of the ‘parent’ heptadiene substrate, despite the *gem*-disubstitution; this order of reactivity was confirmed by a competition RCM experiment (5 mM heptadiene, 5 mM diethyl diallylmalonate, 0.1 mM 1) in which the heptadiene cyclized

**Table 8.** Rate Constants ( $\text{L mol}^{-1} \text{s}^{-1}$ ) Obtained from Batch Fitting Data Sets

entry	$k_{-1}^{\text{G}2}$	$k_1^{\text{GH}2}$	$k_2^5$	$k_{-2}^5$	$k_2^6$	$k_{-2}^6$
1	984	N/A	224	$1.44 \times 10^{-6}$	405	8.28
2	789	$8.89 \times 10^{-5a}$	200	0.0511	426	0.0136
3	22.7	$0.0234^b$	83.6	6.69		

<sup>a</sup>Units  $\text{s}^{-1}$ . <sup>b</sup>Measured by following the reaction of **2** with ethyl vinyl ether in chloroform at 298 K by UV/vis spectrometry following the experimental procedure in ref 18 and fixed in the fitting.

more rapidly (see the Supporting Information). Small scale RCM experiments at up to  $[\text{7}] = 4 \text{ M}$  showed that despite the fact that **7** undergoes RCM slower than heptadiene **11**, it is a far more efficient reaction (higher  $\text{EM}_{\text{T}}$ )<sup>29</sup> and does not produce oligomeric material even when run almost neat. This is in stark contrast to heptadiene which produces oligomeric material even at concentrations as low as  $10^{-2} \text{ M}$ ,<sup>7</sup> further highlighting the need for a quantitative understanding of the effects of substrate structure on RCM rate and efficiency; trends in RCM rate are not always the same as those in RCM efficiency.<sup>6</sup>

Fitting of a batch of data in chloroform-*d* (**11/13** mixtures, each with 0.1 mM **1**: 10/0, 9/1, 7.5/2.5, 5/5, 2.5/7.5, 1/9, 0/10) with  $k_1$  fixed ( $4.5 \times 10^{-5} \text{ s}^{-1}$ ) yielded a set of rate constants for heptadiene and octadiene RCM in chloroform-*d* (Table 8, entry 1).

Many studies have been conducted to understand the effects of precatalyst on reaction rate and outcome,<sup>17,30</sup> so the ability of the model to predict the effect of changing the precatalyst was investigated. Precatalyst **2** generates the same active species as **1** after the first turnover, so two competition reactions (in duplicate in chloroform-*d* with either 0.1 mM **1** or 0.1 mM **2**, plus 5 mM heptadiene and 5 mM octadiene) were conducted and the data were imported into Berkeley Madonna.

The four experiments were fitted with common  $k_2^5$ ,  $k_{-2}^5$ ,  $k_2^6$  and  $k_{-2}^6$  (forward and backward rates for heptadiene and octadiene respectively, the superscript refers to the product ring size) with  $k_1^{\text{G}2}$  and  $k_{-1}^{\text{G}2}$  to model the behavior of **1** and  $k_1^{\text{GH}2}$  to model the initiation of **2**; although the initiation of **2** has been shown to proceed *via* an interchange mechanism,<sup>19,20</sup> a dissociative mechanism (the simplest model) was trialed first to see if a correctly shaped concentration/time plot could be generated. Fitting the data ( $k_3$  fixed to zero) yielded a set of rate constants similar to those obtained for the various chloroform/**1** data (Table 8, entry 1) that approximately described the data from reactions with **1** but more accurately described the octadiene/cyclohexene profiles from reactions with **2** (Table 8, entry 2). Recently, the timing of events involved in the initiation of Grubbs-Hoveyda second generation precatalyst **2** has been re-evaluated. Vorfalt et al. have recently shown that precatalyst initiation is irreversible,<sup>31</sup> in disagreement with the more established “boomerang” mechanism previously proposed.<sup>32</sup>

Modifying the way in which the initiation behavior is modeled for **2** may therefore be appropriate; an interchange mechanism, (eqs 7–12) was therefore explored.

$$\frac{d}{dt}[\text{2}] = k_1^{\text{GH}2}[\text{2}][\text{11}] - k_1^{\text{GH}2}[\text{2}][\text{13}] \quad (7)$$

$$\frac{d}{dt}[\text{9}] = k_1^{\text{GH}2}[\text{2}][\text{11}] + k_1^{\text{GH}2}[\text{2}][\text{13}] \quad (8)$$

$$\frac{d}{dt}[\text{11}] = k_1^{\text{GH}2}[\text{2}][\text{11}] - k_2[\text{9}][\text{11}] + k_{-2}[\text{9}][\text{12}] \quad (9)$$

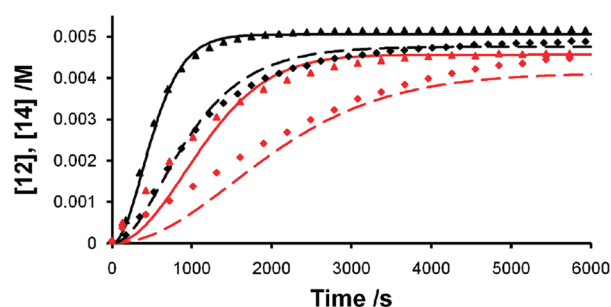


**Figure 8.** Experimental data points and simulated concentration/time profiles for the RCM reactions of a 5 mM/5 mM solution of **11** and **13** with either **1** (red  $\blacktriangle$  = data points for **14**; solid red line = simulation of **14**, red  $\blacklozenge$  = data points for **12**, dashed red line = simulation of **12**) or **2** ( $\blacktriangle$ , solid black line and  $\blacklozenge$ , dashed black line); diamonds/dashed lines represent **12** and triangles/solid lines represent **14**.

$$\frac{d}{dt}[\text{12}] = k_1^{\text{GH}2}[\text{2}][\text{11}] + k_2[\text{9}][\text{11}] - k_{-2}[\text{9}][\text{12}] \quad (10)$$

$$\frac{d}{dt}[\text{13}] = k_1^{\text{GH}2}[\text{2}][\text{13}] - k_2[\text{9}][\text{13}] + k_{-2}[\text{9}][\text{14}] \quad (11)$$

$$\frac{d}{dt}[\text{14}] = k_1^{\text{GH}2}[\text{2}][\text{13}] + k_2[\text{9}][\text{13}] - k_{-2}[\text{9}][\text{14}] \quad (12)$$

The model was set up to allow simulation of RCM of binary mixtures of dienes **11** and **13** with **2**, and to see how the model behaved for data obtained with **1**. Values of  $k_1$  obtained from initiation kinetics were fixed in the simulations. Values of  $k_2^5$ ,  $k_{-2}^5$ ,  $k_2^6$ ,  $k_{-2}^6$  and  $k_{-1}$  were allowed to vary (Table 8, entry 3). The fitting was quite successful for **2**, though less successful for **1**; the exact shape of concentration/time profile cannot be simulated (Figure 8).

It does not appear that the same model can be used for both precatalysts, which may suggest strongly that there are significant mechanistic differences between the processes involving **1** and **2**. Nevertheless, these initial successes for the simulation for the interchange mechanism are extremely promising.

## CONCLUSIONS

We have found that the kinetic model published by Adjiman and Taylor significantly simplifies the canonical mechanism for RCM at some cost. Specifically, the treatment of the ruthenium species is not detailed enough, the precatalyst initiation rates obtained in the original paper through data fitting are inconsistent with literature knowledge, the prediction of active catalyst concentration is incorrect, and ethene is not considered at all. Consequently the model does not describe even a modest range of substrate concentrations well. However, when constrained with measured initiation rate constants, concentration/time profiles can be simulated accurately, albeit over relatively narrow (*ca.* 100 to 300 mM) concentration ranges, and changes in precatalyst loading can be described. Pleasingly, from kinetic experiments on different substrates (at a common concentration, and with a constant  $k_1/k_{-1}$  in the fitting), relative rates can be extracted, and thus useful quantitative performance comparisons can be made between RCM substrates. Unfortunately, it is not possible to use a common model for accurate simulation with precatalysts **1** and **2**, consistent with recent findings on the mechanism of initiation of **2**.



These studies show the need for the development of a more robust modeling approach for RCM if kinetic data are to be interpreted successfully and fully. We are currently working on further development and elaboration of these models for applications over wider concentration ranges and with different precatalysts.

## EXPERIMENTAL SECTION

Kinetics experiments were followed by  $^1\text{H}$  NMR, either by observation at 400 MHz with a BBFO-*z*-ATMA probe or at 600 MHz with a TBI-*z* probe (inverse probe). Both instruments possess temperature control units which maintained the samples at 298 K throughout. All kinetics experiments were conducted in NMR tubes fitted with pierced caps.

Solutions for kinetics experiments were prepared using methods similar to those reported previously.<sup>8</sup> Glove box conditions were not employed, but the precatalysts and solutions thereof were handled with care under nitrogen. All solutions were prepared in dry volumetric glassware and carefully transferred using dry gastight syringes. DCM-*d*<sub>2</sub> was purchased from Goss Scientific and chloroform-*d* from Sigma-Aldrich; solvents were dried on activated 4 Å molecular sieves for at least 24 h before use. The internal standard (1,3,5-trimethoxybenzene) and precatalysts **1** and **2** were purchased from Sigma-Aldrich and used as supplied.

For low concentration reactions, the substrate/internal standard solution was used to tune, match, lock and shim the instrument. A small (*ca.* 5 to 20  $\mu\text{L}$ ) volume of a concentrated precatalyst solution was added and the tube was shaken. For higher concentration reactions the substrate/internal standard solution and precatalyst solution were prepared, a "*t*<sub>0</sub>" sample was prepared from *x*  $\mu\text{L}$  solvent plus (500 - *x*)  $\mu\text{L}$  substrate/standard solution and this was used to prepare the instrument and acquire the first spectrum. Following this, in a separate tube, *x*  $\mu\text{L}$  precatalyst solution was added to (500 - *x*)  $\mu\text{L}$  substrate/standard solution and the tube was shaken.

NMR spectra were then acquired periodically until after the RCM reaction had finished; a D<sub>1</sub> setting of 35 s was used (5 times the largest T<sub>1</sub> measured: 7 s, see Supporting Information). Spectra were processed using proprietary software.<sup>33</sup>

## ASSOCIATED CONTENT

**S** Supporting Information. Kinetic data, sample spectra, rate constants and simulated profiles from data-fitting. This material is available free of charge via the Internet at <http://pubs.acs.org>.

## AUTHOR INFORMATION

### Corresponding Author

\*[jonathan.percy@strath.ac.uk](mailto:jonathan.percy@strath.ac.uk)

### Present Addresses

<sup>†</sup>Laboratorio di Scienze dei Materiali e Nanotecnologie (LMNT), D.ADU Università di Sassari, c/o Porto Conte, Ricerche, 07041 Alghero (SS), Sardinia, Italy

## ACKNOWLEDGMENT

We thank Dr. John Parkinson and Mr. Craig Irving for assistance with NMR experiments and Mr. Gavin Bain for Karl Fischer titrimetric measurements. We thank AstraZeneca (Industrial CASE to D.J.N.) and the EPSRC Initiative in Physical Organic Chemistry 2 (EP/G013160/1 and EP/G013020/1, fellowship to D.C.) for funding.

## REFERENCES

- (1) Hoveyda, A. H.; Zhugralin, A. R. *Nature* **2007**, *450*, 243.
- (2) Yee, N. K.; Farina, V.; Houpis, I. N.; Haddad, N.; Frutos, R. P.; Gallou, F.; Wang, X.-J.; Wei, X.; Simpson, R. D.; Feng, X.; Fuchs, V.; Xu, Y.; Tan, J.; Zhang, L.; Xu, J.; Smith-Keenan, L. L.; Vitous, J.; Ridges, M. D.; Spinelli, E. M.; Johnson, M.; Donsbach, K.; Nicola, T.; Brenner, M.; Winter, E.; Kreye, P.; Samstag, W. *J. Org. Chem.* **2006**, *71*, 7133.
- (3) Shu, C.; Zeng, X.; Hao, M.-H.; Wei, X.; Yee, N. K.; Busacca, C. A.; Han, Z.; Farina, V.; Senanayake, C. H. *Org. Lett.* **2008**, *10*, 1303.
- (4) Farina, V.; Shu, C.; Zeng, X.; Wei, X.; Han, Z.; Yee, N. K.; Senanayake, C. H. *Org. Process Res. Dev.* **2009**, *13*, 250.
- (5) Ercolani, G.; Mandolini, L.; Mencarelli, P.; Roelens, S. *J. Am. Chem. Soc.* **1993**, *115*, 3901.
- (6) Mitchell, L.; Parkinson, J. A.; Percy, J. M.; Singh, K. *J. Org. Chem.* **2008**, *73*, 2389.
- (7) Nelson, D. J.; Ashworth, I. W.; Hillier, I. H.; Kyne, S. H.; Pandian, S.; Parkinson, J. A.; Percy, J. M.; Rinaudo, G.; Vincent, M. A. *Chem. Eur. J.* **2011**, DOI: 10.1002/chem.201101662.
- (8) Ashworth, I. W.; Carboni, D.; Hillier, I. H.; Nelson, D. J.; Percy, J. M.; Rinaudo, G.; Vincent, M. A. *Chem. Commun.* **2010**, *46*, 7145.
- (9) Hillier, I. H.; Pandian, S.; Percy, J. M.; Vincent, M. A. *Dalton Trans.* **2011**, *40*, 1061.
- (10) Adjiman, C. S.; Clarke, A. J.; Cooper, G.; Taylor, P. C. *Chem. Commun.* **2008**, 2806.
- (11) Wieberg, K. B. In *Techniques of Chemistry*; Lewis, E. S., Ed.; Wiley: New York, 1974.
- (12) Zahnley, T.; Macey, R.; Oster, G. In *Berkeley Madonna*, 8.3.18 ed.; University of California at Berkeley: Berkeley, CA, 2010.
- (13) In *Micromath Scientist*, 3.0 ed.; Micromath: St. Louis, MO, 2011.
- (14) Butcher, J. C. *Numerical Methods for Ordinary Differential Equations*; Wiley: Chichester, 2003.
- (15) Ritter, T.; Hejl, A.; Wenzel, A. G.; Funk, T. W.; Grubbs, R. H. *Organometallics* **2006**, *25*, 5740.
- (16) Dias, E. L.; Nguyen, S. T.; Grubbs, R. H. *J. Am. Chem. Soc.* **1997**, *119*, 3887.
- (17) Stewart, I. C.; Keitz, B. K.; Kuhn, K. M.; Thomas, R. M.; Grubbs, R. H. *J. Am. Chem. Soc.* **2010**, *132*, 8534.
- (18) Sanford, M. S.; Love, J. A.; Grubbs, R. H. *J. Am. Chem. Soc.* **2001**, *123*, 6543.
- (19) Vorfalt, T.; Wannowius, K. J.; Plenio, H. *Angew. Chem., Int. Ed.* **2010**, *49*, 5533.
- (20) Ashworth, I. W.; Hillier, I. H.; Nelson, D. J.; Percy, J. M.; Vincent, M. A. *Chem. Commun.* **2011**, *47*, 5428.
- (21) Tsipis, A. C.; Orpen, A. G.; Harvey, J. N. *Dalton Trans.* **2005**, 2849.
- (22) Torker, S.; Merki, D.; Chen, P. *J. Am. Chem. Soc.* **2008**, *130*, 4808.
- (23) Hong, S. H.; Day, M. W.; Grubbs, R. H. *J. Am. Chem. Soc.* **2004**, *126*, 7414.
- (24) Hong, S. H.; Wenzel, A. G.; Salguero, T. T.; Day, M. W.; Grubbs, R. H. *J. Am. Chem. Soc.* **2007**, *129*, 7961.
- (25) Scholl, M.; Ding, S.; Lee, C. W.; Grubbs, R. H. *Org. Lett.* **1999**, *1*, 953.
- (26) Love, J. A.; Sanford, M. S.; Day, M. W.; Grubbs, R. H. *J. Am. Chem. Soc.* **2003**, *125*, 10103.
- (27) van der Eide, E. F.; Piers, W. E. *Nat. Chem.* **2010**, *2*, 571.
- (28) Romero, P. E.; Piers, W. E. *J. Am. Chem. Soc.* **2005**, *127*, 5032.
- (29) Kirby, A. J. *Adv. Phys. Org. Chem.* **1980**, *17*, 183.
- (30) Bieniek, M.; Michrowska, A.; Usanov, D. L.; Grela, K. *Chem.—Eur. J.* **2008**, *14*, 806.
- (31) Vorfalt, T.; Wannowius, K. J.; Thiel, V.; Plenio, H. *Chem.—Eur. J.* **2010**, *16*, 12312.
- (32) Kingsbury, J. S.; Harrity, J. P. A.; Bonitatebus, P. J.; Hoveyda, A. H. *J. Am. Chem. Soc.* **1999**, *121*, 791.
- (33) *Topspin*, 2.1 ed.; Bruker: Billerica, MA, 2007.